Journal of Materials Chemistry C

PAPER

View Article Online
View Journal | View Issue

Cite this: J. Mater. Chem. C, 2018, 6, 13232

A highly sensitive and flexible capacitive pressure sensor based on a micro-arrayed polydimethylsiloxane dielectric layer†

Longquan Ma,[ab] Xingtian Shuai,[a] Yougen Hu,[a] Xianwen Liang,[ac] Pengli Zhu,* [a] Rong Sun [a] and Ching-ping Wong [d]

Received 28th August 2018,
Accepted 15th November 2018

DOI: 10.1039/c8tc04297g

rsc.li/materials-c

A flexible pressure sensor with high sensitivity has been proposed which consists of a typical sandwich structure by integrating a polydimethylsiloxane (PDMS) substrate with a micro-arrayed PDMS dielectric layer. A PDMS flexible substrate coated with silver nanowires (AgNWs) is used as a top/bottom electrode material, and a PDMS dielectric layer with micro-array structure is used to ensure high sensitivity of the pressure sensor. As a result, compared with conventional parallel board capacitive sensors, such sensors exhibit good performance, high sensitivity (2.04 kPa^{-1}) in low pressure ranges (0–2000 Pa), low detection limits (<7 Pa) and fast response times (<100 ms). Furthermore, the integration of the sensor electrode and the dielectric layer ensures good bending stability and cycling stability of the sensor. Flexible capacitive pressure sensors can be used to measure the pressure distribution of finger tips when holding an object and grabbed with fingers. The spatial distribution of the applied pressure can also be clearly identified by fabricating a pressure sensor array. Due to its outstanding performance, the flexible pressure sensor shows bright application prospects in wearable sensing devices, electronic skins and humanoid robotics.

Introduction

In recent years, highly sensitive and flexible pressure sensors have gained great attention because of their growing demand in the field of flexible electronic devices, such as wearable sensing devices,[1–4] biomedical diagnostics,[5,6] electronic skins[7,8] and soft robotics.[9,10] In order to make the above technology better applied in industrial production and human life, flexible pressure sensors with low manufacturing cost, simple processing and high performance are urgently required. Currently, a variety of pressure sensors have been prepared with different sensing mechanisms,[11] mainly divided into the following four categories: capacitive,[12,13] piezoresistive,[14] piezoelectric,[15] and triboelectric.[16] Among them, capacitive pressure sensors[17,18] and piezoresistive pressure sensors[19–21] have advantages such as simple manufacture, low cost and high stability, *etc.*, but in comparison, capacitive pressure sensors have a higher sensitivity and adjustability, and have received more and more attention.

A flexible capacitive pressure sensor can be regarded as a kind of parallel plate capacitor. The main structure of the capacitive pressure sensor consists of two parts: top/bottom electrodes and an intermediate insulating dielectric layer. Since the structure of the sensor is stable, the pressure sensor has high stability, but the sensitivity is not high enough. Sensitivity is one of the most important parameters for measuring sensor performance. The capacitance (C) value of the capacitive pressure sensor depends on the space between the two electrodes (d), the relative effective ratio of the two electrodes, and the relative dielectric constant (ε_r). And the change in capacitance at a certain pressure range (*i.e.*, sensitivity) is closely related to the structure of the top/bottom electrode of the sensor and the dielectric constant of the dielectric layer. The electrode is commonly prepared by using a flexible polymer substrate and a kind of conductive filler to ensure the flexibility of the sensor. The dielectric layer usually uses a polymer with a large dielectric constant to improve the sensitivity of the sensor. For example, PDMS, polyurethane (PU) and polyimide (PI) are the most popular polymer substrates,[22–24] while carbon nanotubes, graphene, metal particles and metal nanowires are the commonly used conductive fillers.[14,25–28] Polyvinylidene fluoride (PVDF), polyvinylpyrrolidone (PVP) and Ecoflex silicone elastomers, *etc.*[5,29,30] which have high dielectric

[a] Shenzhen Institutes of Advanced Technology, Chinese Academy of Sciences, Shenzhen 518005, China. E-mail: pl.zhu@siat.ac.cn
[b] College of Materials Science and Engineering, Shenzhen University, Shenzhen 518060, China
[c] Shenzhen College of Advanced Technology, University of Chinese Academy of Sciences, Shenzhen 518055, P. R. China
[d] School of Materials Science and Engineering, Georgia Institute of Technology, Atlanta, USA

† Electronic supplementary information (ESI) available. See DOI: 10.1039/c8tc04297g

constants, are mostly used as the dielectric layer for the capacitive pressure sensor. In order to improve the sensitivity of the capacitive sensor and its related performance, the electrode or the dielectric layer must have a more obvious deformation under the equal pressure range of change. The most effective method is to achieve electrode microstructure or pore formation of the dielectric layer. The common methods to fabricate a microstructured electrode include chemical etching and photolithography processes.[31,32] However, the preparation process is complex and expensive, and cannot be applied in industrial production. In addition, there are some other preparation methods, such as copying the surface microstructure of the sand paper[25] and replicating the microstructure of a plant surface (lotus leaves, rose petals, *etc.*).[33] The microstructures prepared by the above methods cannot obtain a regular morphology. It is difficult to carry out standardized production, and the performance of the different batches of product is different and not easy to control. As for research on dielectric layers, the following two aspects are mainly involved: firstly, the porosity of the dielectric layer, for example, Chen *et al.*[34] prepared a porous dielectric layer by adding ammonium bicarbonate (NH_4HCO_3) to PDMS, which greatly improves the linear response range of the sensor. In comparison, the microstructure of the dielectric layer is more common. Li *et al.*[17] proposed the use of polystyrene microspheres as the dielectric layer with a sensitivity of 0.815 kPa^{-1}; Bao *et al.*[35] attempted to prepare a dielectric layer of pyramid-shape by using an etched silicon method, while the sensitivity is 0.55 kPa^{-1}. However, introducing a hole in the dielectric layer will inevitably lower the dielectric constant and make the original capacitance smaller, eventually encountering a limit to continue to increase sensitivity. Sharp microstructures also affect stability and linear response at low pressure of the sensor. Therefore, how to improve the comprehensive performance of the capacitive pressure sensor *via* changing the microstructure of the dielectric layer is still an important issue which is worth researching.

Herein, we report a highly sensitive and flexible capacitive pressure sensor with a micro-array structured dielectric layer *via* a simple strategy. A PDMS substrate with AgNWs attached is applied as the top/bottom electrode, and PDMS with a micro-array structure is used as the dielectric layer. The micro-array structure is obtained by plasma treatment under a low-pressure air atmosphere; the pre-stretched PDMS film shows a spontaneous buckle surface structure and is used as the micro-array mold to obtain the micro-arrayed flexible dielectric layer. Subsequently, the obtained micro-array structured dielectric layer and the lower electrode of the sensor are combined by pre-cured PDMS to improve the integration degree of the sensor, and the top electrode is then superimposed to obtain the flexible capacitive pressure sensor. The sensor prepared by the above method has high sensitivity, fast response times, low-pressure detection limits, high bending stability and long-term cycling stability. Furthermore, the capacitive pressure sensor based on the micro-arrayed dielectric layer can be easily extended to obtain a pressure sensor array, which can measure the spatial distribution of the applied pressure.

Experimental

Materials

PDMS feedstock was purchased from Dow Corning, Sylgard 184. AgNWs were prepared *via* a polyol reduction method by ourselves. The PET film was purchased from Toray Corp with a thickness of 200 μm.

Fabrication of the top/bottom electrode

In order to prepare the top/bottom electrode, the PDMS elastomer, a liquid PDMS precursor and a curing agent are mixed at a mass ratio of 10 : 1, and placed in a vacuum oven to remove the gas mixed during the mixing process. Then, the mixture was spin-coated onto a glass substrate and cured at 75 °C for 2 h. To prepare the AgNW PDMS electrode, 0.01 mg mL^{-1} self-prepared AgNWs/ethanol dispersion was left on filter paper (220 nm pore size) through a filter plant and dried for 1 h at room temperature. After that, the PDMS elastomer was placed on the filter paper with AgNWs and the vacuum pump was kept working to make the AgNW and PDMS elastomers more tightly integrated. Finally, the PDMS elastomer is peeled off with the AgNWs, and an electrode for the size required for the experiment was prepared by cutting.

Preparation of the dielectric layer and pressure sensors

The dielectric layer with a micro-array structure was prepared by the following steps. Firstly, the PDMS elastomer was stretched to 130% using a stretching device, and the stretched PDMS elastomer was treated for 10 min by using plasma etching. Then, the PDMS elastomer is released to the original length to form the micro-array structure. After that, the liquid PDMS mixture was attached onto the micro-array structure PDMS substrate uniformly by spin coating, while the bottom electrode prepared above was coated with liquid PDMS on the side containing the AgNWs. The electrode was placed on the micro-array structure coated with liquid PDMS to stick them together. Then the mixture was cured at 75 °C for 2 h. The cured micro-array structure PDMS dielectric layer and bottom electrode (the two parts have been closely integrated) were peeled off from the buckled mold. Finally, the top PDMS flexible electrode was laminated onto the PDMS flexible bottom electrode with the PDMS micro-array dielectric layer to obtain the capacitive pressure sensor.

Characterization and measurements

The PDMS film was treated using a plasma etching machine (Diener Femto) to obtain the micro-array structure. The microscopy images were identified using a metallographic microscope and a polarizing microscope. The microstructures of the dielectric layer and the electrode were observed by scanning electron microscopy (FEI Nova NanoSEM 450). An Agilent 4280A LCR meter was introduced to get the capacitance. A noncontact sheet resistance tester (Napson EC-80P) was used to measure the sheet resistance. The performance of the pressure sensor was detected using a ZHIQU pressure testing

machine with a *z*-axis motor stage, which can be applied at a desired pressure onto the device.

Results and discussion

The fabrication process of the flexible capacitive pressure sensor mainly includes two parts: (i) the preparation of the PDMS flexible electrode; (ii) the fabrication of the PDMS flexible electrode with a PDMS micro-array structure on the surface as the dielectric layer. Fig. 1 presents the schematic illustration of the detailed manufacturing process of the flexible capacitive pressure sensor. Part one deals with the PDMS flexible electrode prepared using the vacuum filtration method and the peeling-off process. First of all, the as-prepared AgNWs were homogeneously dispersed in ethanol *via* ultrasonication to form an AgNW/ethanol suspension. Subsequently, the obtained suspension was filtered on filter paper, followed by a drying process at room temperature to obtain AgNW thin films. Secondly, the pre-cured PDMS film was placed onto the surface of the AgNW film, and vacuum filtration was applied for binding the PDMS substrate and the AgNWs on filter paper more closely. Finally, the PDMS composite film, where the AgNW film is embodied on the surface and serves as the conducting layer, was obtained by separating the substrate with silver nanowires and filter paper. In this experiment, the amount of silver nanowires on the flexible electrode was 0.02 mg cm^{-2}, and the square resistance of the flexible electrode decreased to 2.75 Ω sq^{-1}. Due to the outstanding flexibility of the PDMS elastomer matrix, the as-prepared PDMS composite film possesses notable flexibility and acts as a PDMS flexible electrode.[7,22]

Part two deals with the fabrication of the PDMS flexible electrode with a PDMS micro-array structure on the surface. Firstly, the cured PDMS film was stretched with a certain strain, and then treated with dry air low-pressure plasma to form a staff silicon oxide (SiO_x) thin layer. When the film was released to the initial status, a series of micro-array structures were generated on its treated surface because of the rigid surface without shrinkage. Secondly, a certain amount of pre-cured PDMS solution was spin-coated onto the treated surface of the PDMS film to transfer the micro-array structure patterning as the dielectric layer. Then the as-prepared PDMS flexible electrode, with the AgNW side downward, was placed and laminated onto the surface of the fresh PDMS film. Thirdly, after the PDMS complex was cured, the PDMS flexible electrode with a PDMS micro-array dielectric layer on the surface was obtained by peeling off from the PDMS micro-array mould. Finally, the capacitive pressure sensor was set up *via* integrating

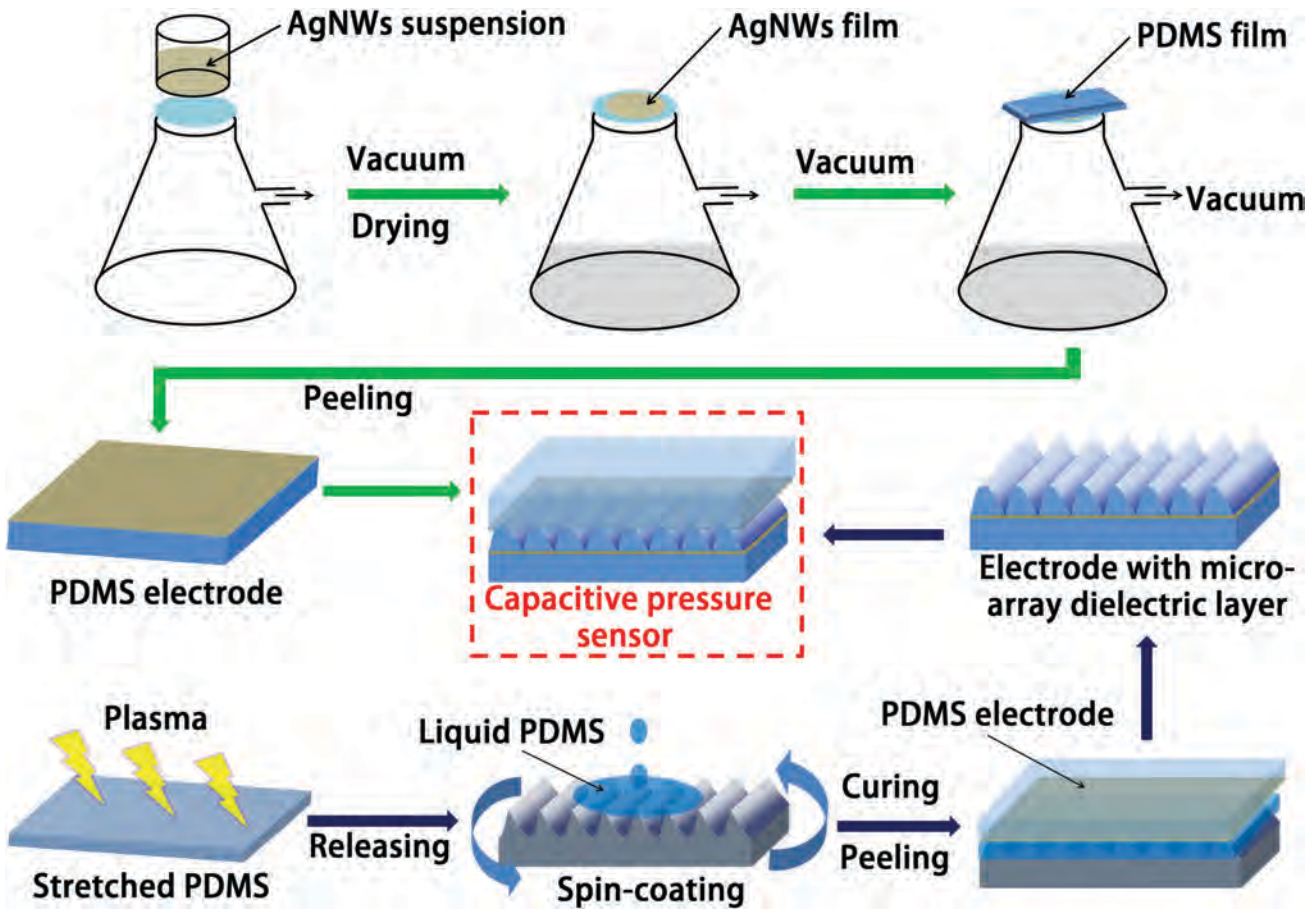

Fig. 1 Fabrication process of the capacitive flexible pressure sensor based on the micro-arrayed PDMS dielectric layer.

the PDMS flexible electrode and the PDMS flexible electrode with the PDMS micro-array structure on the surface, where the AgNW film side in the PDMS flexible electrode and the micro-array dielectric layer side locate in the middle and face each other. In particular, as the PDMS flexible electrode and the PDMS flexible electrode with a micro-array structure on the surface are both fabricated with the flexible PDMS substrate, the integrated capacitive pressure sensor is able to display outstanding flexibility and durability in bending and pressing tests and practical applications. In this article, AgNWs are used as the conductive medium. The conductivity property of the PDMS flexible electrode is largely dependent on the distributions of AgNWs on the surface of the PDMS substrate. Accordingly, we intensively characterized the dispersion status of AgNWs on the surface of the PDMS flexible electrode using a polarizing microscope, a metallographic microscope and a scanning electron microscope (SEM), respectively. Optical microscopy images clearly show that the AgNWs are uniformly distributed on the surface of the PDMS substrate (Fig. S2, ESI†). Besides, Fig. 2a shows the SEM image of AgNWs on the surface of the PMDS flexible electrode. The result reveals that the AgNWs are distributed uniformly, which is consistent with the preceding results from microscopy images. Moreover, the adjacent AgNWs are interlinked with each other, as the local enlarged view of AgNWs shows in the inset. The formation of the cross-linked architecture among the AgNWs constructs interconnected networks, which benefits the improvement of the electrical conductivity of the PDMS flexible electrode.

Next, the surface morphology of the micro-array mold and the PDMS flexible electrode with a PDMS dielectric layer were both thoroughly characterized by SEM. As shown in Fig. 2b, the micro-arrays with wave-type convex structures are successfully generated on the surface of the PDMS substrate, acting as the micro-array mold. These convex structures are distributed uniformly, where the convex structure has a width of about 2.7 μm. Moreover, the surface of the PMDS micro-array is quite smooth, which is conducive to the transfer patterning process. The SEM image of the micro-array dielectric layer is given in Fig. 2c. The micro-array structure on the surface also features wave-type convex structures. Similarly, these convex structures are distributed uniformly and their surfaces are relatively smooth. The distance between the peak points of two adjacent convex structures is about 2.6 μm, as shown in Fig. 2d, which is basically in accordance with the width of one convex structure in the micro-array mold. This indicates that the transfer patterning technology used in this study is feasible and effective, and the obtained micro-array structure can be modulated

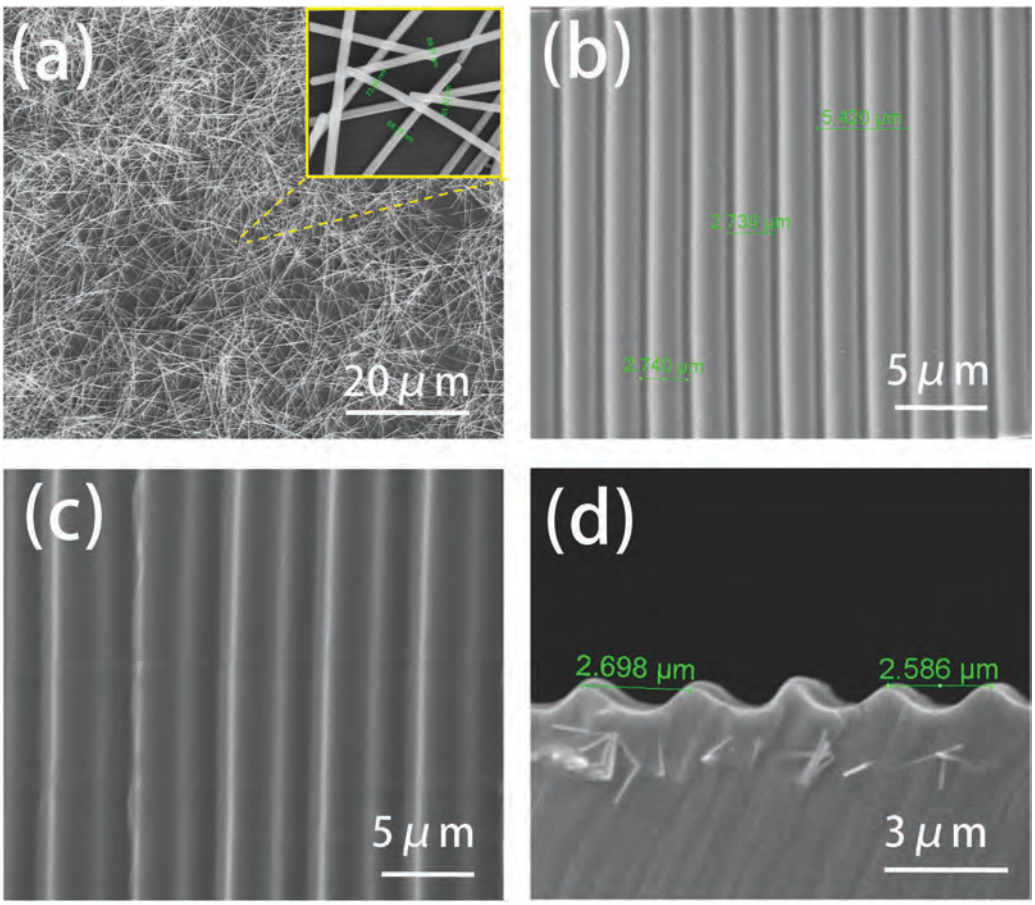

Fig. 2 SEM images of the PDMS flexible electrode and the micro-arrayed PDMS dielectric layer. (a) SEM images of the AgNWs on the flexible PDMS electrode; (b) SEM images of the micro-arrayed PDMS mold; (c) SEM images of the micro-arrayed dielectric layer; and (d) cross-section SEM image of the as-fabricated bottom electrode coated with the micro-arrayed PDMS dielectric layer.

by tuning the structure of the micro-array mold. Fig. 2d presents the SEM image of the cross-sectional morphology of the PDMS flexible electrode, which serves as the dielectric layer. The PDMS with a micro-array structure is successfully generated on the surface of the AgNW film, and highly incorporates with the underneath PDMS flexible electrode substrate. The AgNWs located in the middle, forming a sandwich structure. The PDMS with micro-array structure and AgNWs serve as a dielectric layer and a bottom electrode, respectively. The flexible bottom electrode and the dielectric layer are bonded together and integrally formed to ensure the structural stability of the prepared sensor.

Several important parameters to evaluate the performance of the pressure sensor are pressure sensitivity, hysteresis, detection limit, bending and pressurizing cycling stability, *etc.*[18] In order to investigate the influence of the micro-array structure of the dielectric layer on the performance of the capacitive pressure sensor, an external pressure was applied on both the sensors with the flat dielectric layer and the micro-array structure dielectric layer, respectively. The uniform AgNW electrode is used as the top/bottom electrodes, and the test equipment and conditions are exactly identical. Fig. 3 displays the response characteristics of the flexible pressure sensor based on the PDMS micro-array dielectric layer. Fig. 3a shows the relative capacitance change depending on the pressure of the pressure sensors with the flat dielectric layer and the micro-array dielectric layer, respectively. For using the flat dielectric layer, the pressure sensor exhibits an ultra-low sensitivity of just about 0.01 kPa^{-1} when pressure is applied. Conversely, when the flat dielectric layer was replaced by the micro-array dielectric layer, the sensitivity is improved substantially and two linear parts can be observed clearly in the detection range. One is the low pressure range (0–2000 Pa) with a pressure sensitivity of 2.04 ± 0.16 kPa^{-1}, and the other is the high pressure range (2000–9000 Pa) with a pressure sensitivity of 0.57 ± 0.08 kPa^{-1}. By comparing the pressure sensitivity of the flat dielectric layer based capacitive pressure sensor, the pressure sensitivity of the pressure sensor with the micro-array dielectric layer has a significant improvement. These results manifest that the micro-array structure of the dielectric layer plays a considerable role in improving the sensitivity of the pressure sensor. The preparation of the highly sensitive pressure sensor has always been a common goal. Sensors have a variety of applications in different pressure response ranges. Applications below 10 kPa pressure[36] include ultra-sensitive e-skins, touchscreens, medical diagnosis, daily activities, *etc.* Fig. 3b shows the pressure response curves of the loading and unloading pressures for the consecutive loading–unloading process of the micro-array dielectric layer based pressure sensor. It can be seen that the coincidence of the loading and unloading curves is very high. This means that the pressure sensor has a very small hysteresis. The variation of the flexible pressure sensor before and after

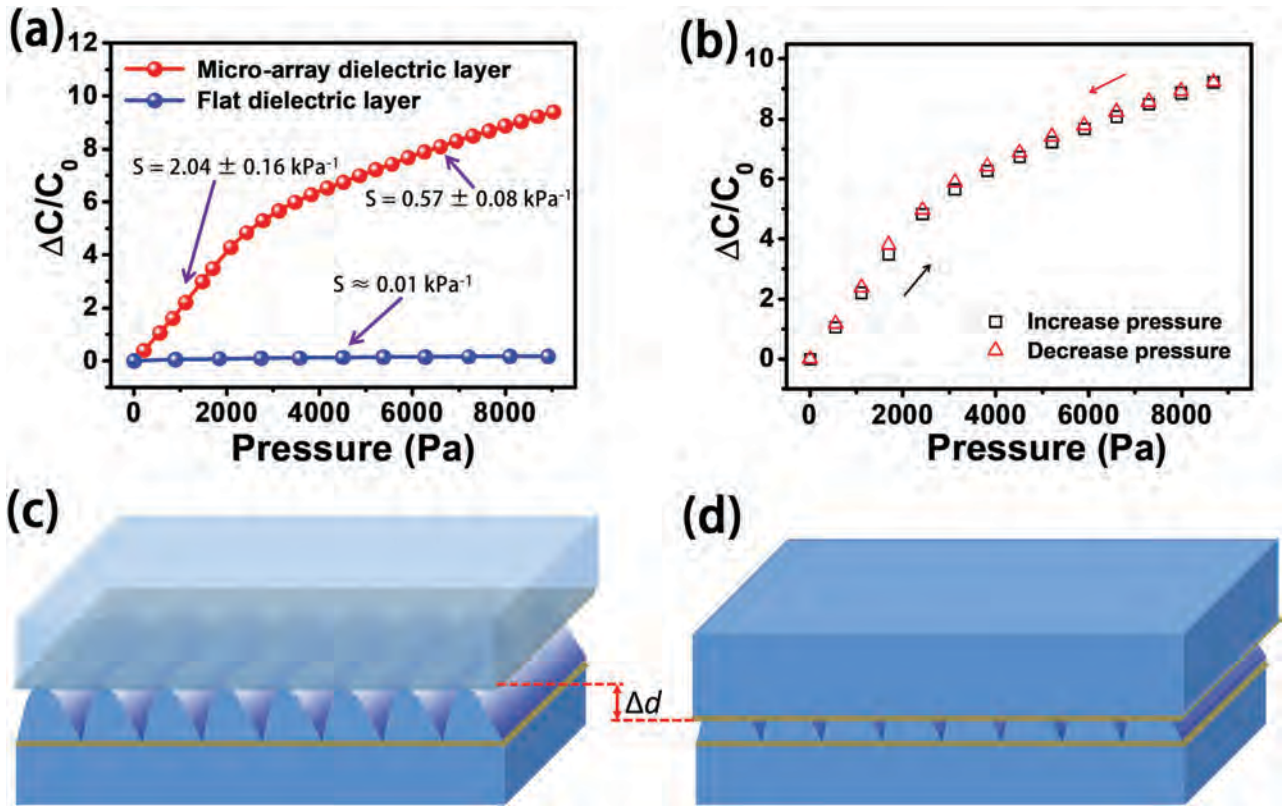

Fig. 3 Response characteristics of the flexible capacitive pressure sensor based on the PDMS micro-array dielectric layer. (a) Relative capacitance change–pressure curves for the capacitive pressure sensors based on the flat dielectric layer and the PDMS micro-array dielectric layer; (b) relative capacitance change–pressure curves from the consecutive loading–unloading cycle; (c) the flexible pressure sensor at the initial state; (d) the pressure sensor after compression deformation.

pressurization is shown in Fig. 3c–d. This high sensitivity of the pressure sensor is closely related to the micro-array structure dielectric layer. The PDMS dielectric layer can be deformed under external pressure and return to the initial state when unloading pressure. According to this feature, the contact area and the distance between the two electrodes will change with the amount of pressure applied. Therefore, when the sensor is pressurized, the contact of the micro-array structure with the top electrode and the deformation of the dielectric layer show a significant increase in the contact area. This can also be seen from the deformation of the cross section when the sensor is under pressure (Fig. S1a–c, ESI†). The distance between the top and bottom electrodes decreases as the applied pressure increases which causes the sensor to exhibit high sensitivity. When the deformation of the micro-array structure is no longer obvious and the air gap is emptied, the sensitivity of the sensor will decrease. Based on the changes in the contact area and the distant between two electrodes, the capacitance value changes rapidly and shows high sensitivity under low pressure. In addition, based on the micro-array structure dielectric layer, the microstructure contains air in the absence of pressure, which should be the reason for the change in sensitivity. In general, the result is that the sensitivity of the sensor is divided into two distinct phases. In the low pressure response range (0–2000 Pa), the volume of the air gap is reduced constantly; when the pressure reaches 2000 Pa, the gap gas is basically drained, so we can clearly see the reduction of the sensitivity in the high pressure range (2000–9000 Pa).

Fig. 4a and its insets show the response times of the capacitive pressure sensor while loading and relaxing pressure on it. When there is no pressure applied onto the sensor, the relative capacitance almost remains without fluctuations, but when a pressure of 2 kPa is instantly pressurized above the flexible pressure sensor at 2.00 s, the relative capacitance increased from 0 to 4.0 immediately at 2.10 s, and then the relative capacitance change remained stable. Conversely, at 4.00 s, when removing the applied pressure, the relative capacitance value returns to the initial state quickly from 4.0 to 0 at 4.10 s. Therefore, this indicates that the response time is less than 100 ms, regardless of the process of applying or releasing pressure on the sensor. When the pressure is loaded onto the sensor, the relative capacitance change in the sensor almost remains unchanged, which means a stable and accurate measurement of the sensor at static pressure.

To investigate the response and stability of the pressure sensor under ultra-low pressure, the sensor was cut into regular squares with a size of 1.0 cm × 1.0 cm. In addition, a mung bean with a small weight (7 Pa) was used as an ultra-low pressure loading object by placing it onto the pressure sensor, which is equal to loading about 7 Pa pressure onto the pressure sensor. The response for the ultra-low pressure from the mung bean was monitored and shown in Fig. 4b. When the mung bean was applied onto the sensor, the average value of the capacitance increased from 4.62 pF to 4.75 pF, and the capacitance change surpasses 0.13 pF, which is large enough to be detected using an Agilent 4280A LCR meter. During the process

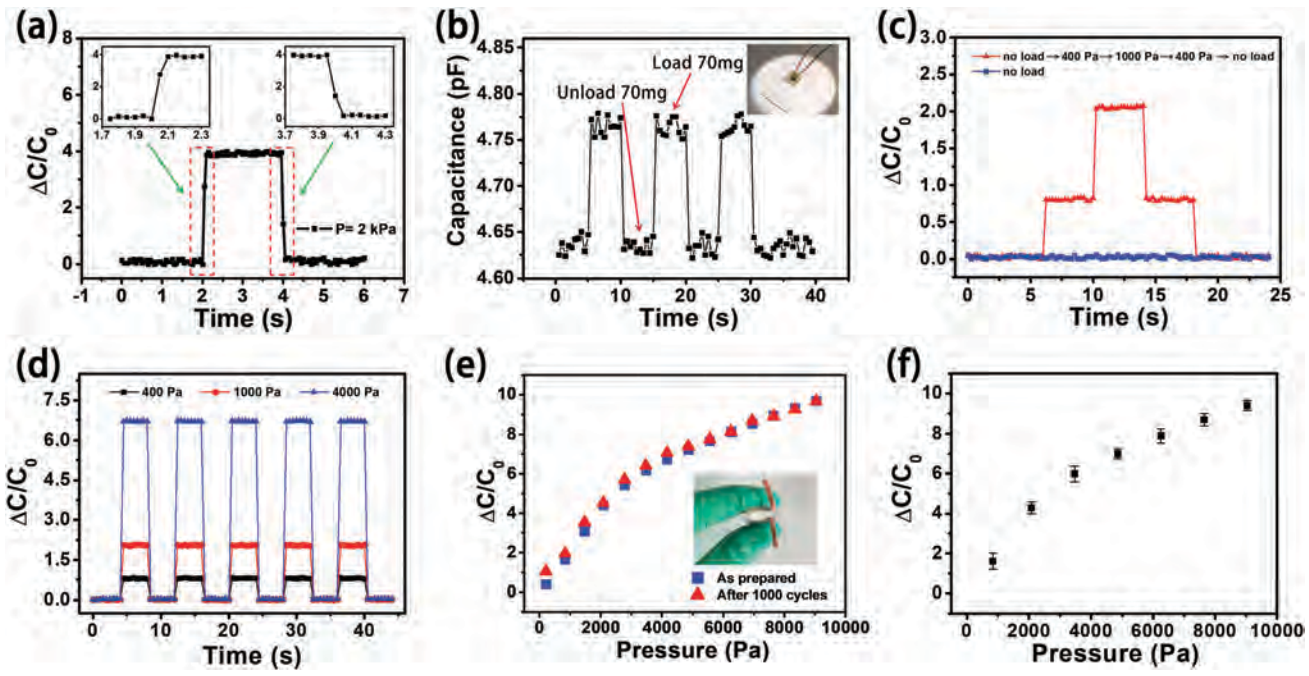

Fig. 4 The performance characterization of the capacitive flexible pressure sensor. (a) Pressure response and relaxation time of the pressure sensor; (b) capacitance–time curve for the detection of ultra-low pressure. (c) Pressure response performance of the capacitive pressure sensor for loading and unloading stair-like pressure at different degrees; (d) pressure response performance of the capacitive pressure sensor for the consecutive seasonal external pressure at various degrees; (e) pressure response of the pressure sensor before and after the 1000-cycle bending test; (f) pressure response of ten independent capacitive pressure sensors.

of the three ultra-low pressure cycling tests, the capacitance response value of each cycle only shows a small change, which explains why the pressure sensor has high stability. Based on the above results, the pressure sensor with the micro-array structured dielectric layer is stable during the multiple loading/unloading cycle tests.

The pressure response performance of the capacitive pressure sensor for loading and unloading stair-like pressure at different degrees was investigated. As shown in Fig. 4c, when a pressure rising and falling just like a stair shape (no load → 400 Pa → 1000 Pa → 400 Pa → no load), was applied onto the pressure sensor, the response and relaxation times were less than 100 ms and the relative capacitance of the pressure sensor showed the same value for the same pressure regardless of the previous pressure. The capacitance value of the pressure sensor is stable at static pressure, which means a perfect performance indicator of the sensor under static pressure and demonstrates the precise measurement for the applied pressure. Subsequently, the pressure response performance of the capacitive pressure sensor for the consecutive seasonal external pressure with various degrees was further investigated, as shown in Fig. 4d. The seasonal external pressures of 400 Pa, 1000 Pa and 4000 Pa were loaded and released onto the capacitive pressure sensor. During the process of loading external pressure at various degrees, the relative capacitance response values of the pressure sensor were 0.78, 2.03, and 6.68, and the pressure sensor almost had noise-free and stable continuous responses for the different external pressures.

Due to the flexible PDMS substrate and the dielectric layer, the pressure sensor also possesses high bending stability. For the bending tests, a PET film (200 μm) was used as a fixture for the capacitive pressure sensor by using tape and bent at a very small curvature radius for 1000 times as shown in the inset of Fig. 4e. The relative capacitance change–pressure curve was recorded at the beginning and after 1000 cycles of bending. Fig. 4e illustrates that the relative capacitance changes in the pressure sensor show no significant change at every applied pressure in comparison with the as-prepared pressure sensor even after the 1000-cycle bending test. In addition, the working stability of the flexible pressure sensor is measured by repeatedly loading a pressure pulse for more than 3000 times and recording the corresponding relative capacitance variation (Fig. S5, ESI†).

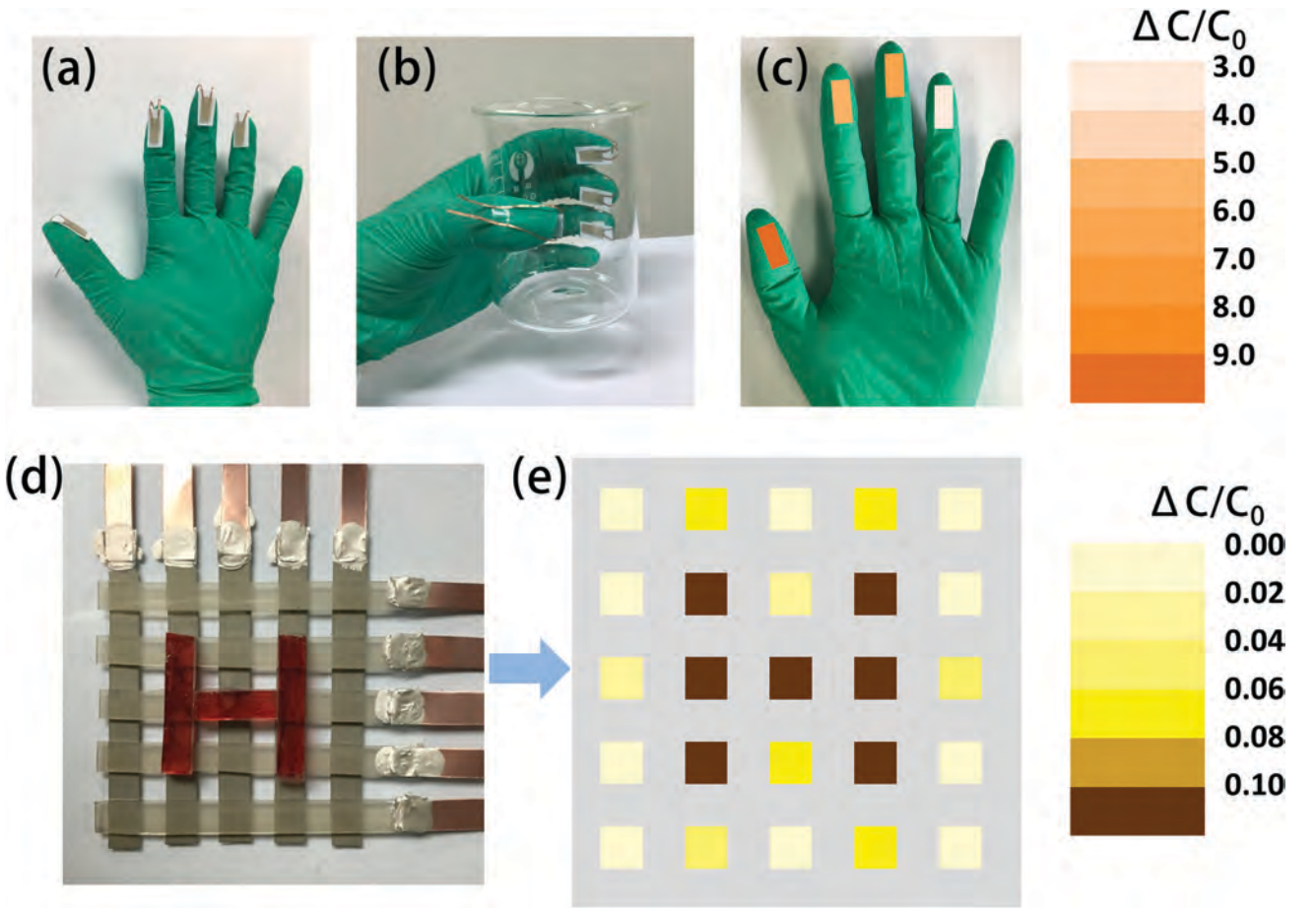

Fig. 5 Fingertip grip pressure sensing device and pressure sensor array based on the flexible capacitive pressure sensor. (a) Photograph of the pressure sensor attached to the fingertips. (b) Photograph of the beaker which was grabbed while the four fingertips with the sensor grip the beaker wall. (c) The corresponding relative capacitance changes of each pressure were collected. The flexible capacitive pressure sensor array with a PDMS mold (260 mg) in the shape of the letter "H" on top (d) and the resulting map of relative capacitance change (e).

The magnitude and frequency of the applied pressure is controlled using a linear motor, and the sensor is fixed onto the platform of the linear motor. By adjusting the height of the platform, the upper substrate of the linear motor generates a compression on the sensor, and the compression frequency is set to 1 Hz. As shown in Fig. S5 (ESI†) and its insets, when the pressure is loaded onto the sensor, the relative capacitance variation increases from 0 to 1.92 and then restores to 0 after unloading the external pressure. During the 3000 repeated pressure cycles, the pressure response value is almost identical for each pressure pulse. The inset exhibits 10 cycles at the beginning and the 3000th cycle of the relative capacitance variations when the external pressure is loaded and unloaded. Even after frequent pressure pulses, the pressure response of the sensor is always stable at 0 (unloading) and 1.92 (loading). The above results show that this flexible pressure sensor still has a stable response after undergoing multiple cyclic pressure pulse tests.

Next, we tested ten pressure sensor samples by comparing the variation in pressure sensitivity between the samples, and Fig. 4f shows the average relative capacitance values under different pressure levels plotted with error bars (standard deviation). It can be observed that the relative capacitance change in each sample approaches the average value under the same pressure, which indicates that the pressure sensor also has high reliability in pressure sensing.

By attaching the sensor to a finger, the flexible pressure sensor can measure the fingertip pressure when holding an object. In order to implement a fingertip pressure sensing device, four fingers except the little finger are labeled with a sensor as shown in Fig. 5a. And all sensors are cut to the same size (6×12 mm^2) to fit onto the fingertips. Then a beaker (102.8 g) was grabbed tightly by the four fingers (Fig. 5b). Fig. 5c shows the amount of pressure, the rate of change in capacitance ($\Delta C/C_0$), applied to the beaker wall by each finger during the holding process. It can be seen that the fingertip of the thumb provides a maximum rate of capacitance change among the four fingers, reaching 9.3, and the ring fingertip has the smallest change rate of capacitance, only 4.1. The other two fingertips, the middle finger and the index finger, have response values of 5.5 and 6.2, respectively. The experimental results demonstrate that the pressure sensor we prepared can be attached to the fingertip to measure the fingertip pressure when holding an object.

It should be understood that the preparation and expansion of the sensor with a micro-array structured dielectric layer is easy. In the process of testing, a pixel-type pressure sensor array was prepared to demonstrate that the sensor could be used to measure the spatial stress distribution. The pixel-type pressure sensor array was formed by cutting the electrode into rectangles and then attaching them onto the PET film (thickness: 50 μm). By cutting the top and bottom electrodes coated with PDMS micro-array dielectric layers of desired size, 5×5 pixel-type sensor arrays were prepared (size of the sensor array is about 30×30 mm^2) and the sizes of each capacitor were 3×3 mm^2. As shown in Fig. 5d, a 260 mg model resembling the letter "H" is placed at the appropriate position on the sensor array. The resulting relative capacitance changes are shown in Fig. 5e, where the yellow color corresponds to a higher capacitance change. The spatial distribution of the applied pressure is clearly expressed.

Conclusions

In summary, we have developed a high sensitivity and flexible capacitive pressure sensor with a micro-array PDMS dielectric layer *via* a simple manufacturing strategy. Due to the good deformation and recovery capability of the micro-array structured PDMS dielectric layer and a higher level of integration, the capacitive pressure sensor exhibits excellent performance. Hence, the pressure sensor exhibits high sensitivities of 2.04 ± 0.16 kPa^{-1} (0–2 kPa) and 0.57 ± 0.08 kPa^{-1} (2–9 kPa) and an ultralow detection limit (<7 Pa). The capacitive pressure sensor shows ultra-short response time (<100 ms). The sensor also possesses high bending stability after a 1000-cycle bending test and high work stability for a multiple pressure cycle test (1000 times). The facile fabrication process can be easily extended to constitute a sensor array that can detect the spatial distribution of the applied pressure. We can also detect the pressure distribution of fingers when grabbing an object. In short, flexible capacitive pressure sensors with inexpensive manufacturing and outstanding performance can be widely applied in wearable sensing devices, electronic skins, and other potential applications.

Conflicts of interest

There are no conflicts to declare.

Acknowledgements

This work was financially supported by the National Natural Science Foundation of China (21571186), the National Key R&D Project from the Ministry of Science and Technology of China (2016YFA0202702), and the R&D Funds for Basic Research Program of Shenzhen (Grant No. JCYJ20150831154213681)

Notes and references

1 T. P. Huynh, P. Sonar and H. Haick, *Adv. Mater.*, 2017, **29**, 1604973.
2 J. Wang, J. Jiu, M. Nogi, T. Sugahara, S. Nagao, H. Koga, P. He and K. Suganuma, *Nanoscale*, 2015, **7**, 2926–2932.
3 Y. Zhang, Y. G. Hu, P. L. Zhu, F. Han, Y. Zhu, R. Sun and C. P. Wong, *ACS Appl. Mater. Interfaces*, 2017, **9**, 35968–35976.
4 B. Wang, T. Shi, Y. Zhang, C. Chen, Q. Li and Y. Fan, *J. Mater. Chem. C*, 2018, **6**, 6423–6428.
5 Z. Z. Ming, X. Ruan, C. Y. Bao, Q. N. Lin, Y. Yang and L. Y. Zhu, *Adv. Funct. Mater.*, 2017, **27**, 1606258.
6 G. Schwartz, B. C. Tee, J. Mei, A. L. Appleton, D. H. Kim, H. Wang and Z. Bao, *Nat. Commun.*, 2013, **4**, 1859.

7 Y. Joo, J. Byun, N. Seong, J. Ha, H. Kim, S. Kim, T. Kim, H. Im, D. Kim and Y. Hong, *Nanoscale*, 2015, **7**, 6208–6215.
8 Z. Wang, Y. Huang, J. Sun, Y. Huang, H. Hu, R. Jiang, W. Gai, G. Li and C. Zhi, *ACS Appl. Mater. Interfaces*, 2016, **8**, 24837–24843.
9 S. Wang, J. Xu, W. Wang, G. N. Wang, R. Rastak, F. Molina-Lopez, J. W. Chung, S. Niu, V. R. Feig, J. Lopez, T. Lei, S. K. Kwon, Y. Kim, A. M. Foudeh, A. Ehrlich, A. Gasperini, Y. Yun, B. Murmann, J. B. Tok and Z. Bao, *Nature*, 2018, **555**, 83–88.
10 S. Park, K. Mondal, R. M. Treadway, V. Kumar, S. Y. Ma, J. D. Holbery and M. D. Dickey, *ACS Appl. Mater. Interfaces*, 2018, **10**, 11261–11268.
11 Y. Khan, A. E. Ostfeld, C. M. Lochner, A. Pierre and A. C. Arias, *Adv. Mater.*, 2016, **28**, 4373–4395.
12 S. W. Lee, S. H. Cho, H. S. Kang, G. Kim, J. S. Kim, B. Jeong, E. H. Kim, S. Yu, I. Hwang, H. Han, T. H. Park, S. H. Jung, J. K. Lee, W. Shim and C. Park, *ACS Appl. Mater. Interfaces*, 2018, **10**, 13757–13766.
13 X. Wang, Z. Liu and T. Zhang, *Small*, 2017, **13**, 1602790.
14 J. Shi, L. Wang, Z. Dai, L. Zhao, M. Du, H. Li and Y. Fang, *Small*, 2018, **14**, 1800819.
15 X. Chen, X. Li, J. Shao, N. An, H. Tian, C. Wang, T. Han, L. Wang and B. Lu, *Small*, 2017, **13**, 1604245.
16 Y. Ma, Q. Zheng, Y. Liu, B. Shi, X. Xue, W. Ji, Z. Liu, Y. Jin, Y. Zou, Z. An, W. Zhang, X. Wang, W. Jiang, Z. Xu, Z. L. Wang, Z. Li and H. Zhang, *Nano Lett.*, 2016, **16**, 6042–6051.
17 T. Li, H. Luo, L. Qin, X. Wang, Z. Xiong, H. Ding, Y. Gu, Z. Liu and T. Zhang, *Small*, 2016, **12**, 5042–5048.
18 X. Shuai, P. Zhu, W. Zeng, Y. Hu, X. Liang, Y. Zhang, R. Sun and C. P. Wong, *ACS Appl. Mater. Interfaces*, 2017, **9**, 26314–26324.
19 Y. A. Samad, K. Komatsu, D. Yamashita, Y. Li, L. Zheng, S. M. Alhassan, Y. Nakano and K. Liao, *Sens. Actuators, B*, 2017, **240**, 1083–1090.
20 B. C. Tee, C. Wang, R. Allen and Z. Bao, *Nat. Nanotechnol.*, 2012, **7**, 825–832.
21 Y. A. Samad, Y. Li, A. Schiffer, S. M. Alhassan and K. Liao, *Small*, 2015, **11**, 2380–2385.
22 X. Qian, Z. Cai, M. Su, F. Li, W. Fang, Y. Li, X. Zhou, Q. Li, X. Feng, W. Li, X. Hu, X. Wang, C. Pan and Y. Song, *Adv. Mater.*, 2018, **30**, e1800291.
23 R. Xu, Y. Lu, C. Jiang, J. Chen, P. Mao, G. Gao, L. Zhang and S. Wu, *ACS Appl. Mater. Interfaces*, 2014, **6**, 13455–13460.
24 Q. T. Zhou, J. G. Park, K. N. Kim, A. K. Thokchom, J. Bae, J. M. Baik and T. Kim, *Nano Energy*, 2018, **48**, 471–480.
25 Y. Pang, K. Zhang, Z. Yang, S. Jiang, Z. Ju, Y. Li, X. Wang, D. Wang, M. Jian, Y. Zhang, R. Liang, H. Tian, Y. Yang and T. L. Ren, *ACS Nano*, 2018, **12**, 2346–2354.
26 T. Yamada, Y. Hayamizu, Y. Yamamoto, Y. Yomogida, A. Izadi-Najafabadi, D. N. Futaba and K. Hata, *Nat. Nanotechnol.*, 2011, **6**, 296–301.
27 P.-N. Ni, C.-X. Shan, S.-P. Wang, X.-Y. Liu and D.-Z. Shen, *J. Mater. Chem. C*, 2013, **1**, 4445–4449.
28 H. Liu, Y. Li, K. Dai, G. Zheng, C. Liu, C. Shen, X. Yan, J. Guo and Z. Guo, *J. Mater. Chem. C*, 2016, **4**, 157–166.
29 S. Garain, S. Jana, T. K. Sinha and D. Mandal, *ACS Appl. Mater. Interfaces*, 2016, **8**, 4532–4540.
30 P. P. Lei, R. An, P. Zhang, S. Yao, S. Y. Song, L. L. Dong, X. Xu, K. M. Du, J. Feng and H. J. Zhang, *Adv. Funct. Mater.*, 2017, **27**, 1702018.
31 B. Nie, X. Li, J. Shao, X. Li, H. Tian, D. Wang, Q. Zhang and B. Lu, *ACS Appl. Mater. Interfaces*, 2017, **9**, 40681–40689.
32 S.-J. Woo, J.-H. Kong, D.-G. Kim and J.-M. Kim, *J. Mater. Chem. C*, 2014, **2**, 4415–4422.
33 J. N. Wang, Y. Q. Liu, Y. L. Zhang, J. Feng, H. Wang, Y. H. Yu and H. B. Sun, *Adv. Funct. Mater.*, 2018, **28**, 1800625.
34 S. Chen, B. Zhuo and X. Guo, *ACS Appl. Mater. Interfaces*, 2016, **8**, 20364–20370.
35 S. C. Mannsfeld, B. C. Tee, R. M. Stoltenberg, C. V. Chen, S. Barman, B. V. Muir, A. N. Sokolov, C. Reese and Z. Bao, *Nat. Mater.*, 2010, **9**, 859–864.
36 Y. Zang, F. Zhang, C.-a. Di and D. Zhu, *Mater. Horiz.*, 2015, **2**, 140–156.

